A natural compound obtained from *Valeriana jatamansi* selectively inhibits glioma stem cells

SHI-GANG QI[1*], LI-QIU QUAN[2*], XIAO-YUE CUI[1], HONG-MEI LI[2], XU-DONG ZHAO[1] and RONG-TAO LI[2]

[1]Key Laboratory of Animal Models and Human Disease Mechanisms of Chinese Academy of Sciences and Yunnan Province, Kunming Institute of Zoology, Chinese Academy of Sciences, Kunming, Yunnan 650223; [2]Faculty of Life Science and Technology, Kunming University of Science and Technology, Kunming, Yunnan 650500, P.R. China

Received December 14, 2018; Accepted October 22, 2019

DOI: 10.3892/ol.2019.11239

Abstract. Glioblastoma is one of the most malignant tumors with very poor prognosis. Glioma stem cells (GSCs) occupy a small proportion in glioma, but they are closely associated with radiotherapy and chemotherapy resistance, promoting tumor angiogenesis, hypoxia response, invasion and recurrence. Therefore, GSCs have become a new target for tumor treatment and are used in drug screening. Rupesin E is a natural compound obtained from *Valeriana jatamansi*, and its antitumor activity has not been reported. In the present study, the antitumor activity of rupesin E was investigated, and the results demonstrated that it inhibited the proliferation of GSCs (GSC-3#, GSC-12#, GSC-18#) with the IC_{50} values of 7.13±1.41, 13.51±1.46 and 4.44±0.22 μg/ml, respectively. In addition, immunofluorescence cell staining and flow cytometry techniques demonstrated that rupesin E inhibited GSC proliferation and induced apoptosis. Furthermore, rupesin E inhibited the ability of GSC colony formation, indicating its antitumor activity against GSCs *in vitro*.

Introduction

Glioblastoma multiforme (GBM) is the most common and lethal malignant primary brain tumor in the world, accounting for 14% of primary brain and other central nervous system tumors (1). The degree of malignancy is reflected by the uncontrollable cell proliferation, high invasiveness, lack of apoptosis and increased angiogenesis (2). The tumor is located under the cortex and most of it occurs throughout the upper cerebral hemisphere; the frontal lobe is the most common site of occurrence (2). According to World Health Organization classification in 2007, GBM was subcategorized as a grade IV tumor (1), which is the highest level in brain tumors. The median survival of patients with GBM is 14 months and only 10% of patients survive >5 years, which suggests that the prognosis is poor (3). In Europe, glioblastoma accounts for 49% of gliomas, and almost 3,000 new cases are diagnosed every year (4). Patients with glioblastoma are mostly elderly, and ~30% of them are ≥70 years old. Currently, the treatment for glioblastoma is surgery combined with radiotherapy and chemotherapy or adjuvant therapy (chemotherapy) with temozolomide. Although surgical resection can effectively reduce intracranial pressure, it can also cause postoperative cerebral edema and the incidence of neurological complications (5). However, as glioblastoma has a diffuse infiltration and growth pattern, if a portion of the tumor is located in important functional areas, such as language or motor centers, in order not to aggravate the dysfunction of brain function, the majority of tumors can only be partially resected and cannot be completely separated from normal brain tissue (5). Although radiotherapy can work against tumor cells of great quantity, radiation also causes damage to normal brain tissue, and multiple treatments can lead to glioblastoma developing tolerance (6). It has previously been reported that the radioresistance of glioblastoma is mainly associated with DNA damage repair mechanisms in GSCs (6). Although chemotherapy can effectively treat the tumor, after long-term use, tumor cells also develop resistance (7-9); solving drug resistance of the tumor is a difficult problem in glioblastoma treatment, and a large number of studies have been performed to identify potential solutions.

Since cancer stem cells, known as tumor-initiating cells (TICs), were first identified in acute myelogenous leukemia (10), tumor stem cells have become a hotspot of research. In numerous types of tumor tissues, such as myeloma, lung cancer and ovarian cancer, a small number of cells have the ability of self-renewal, infinite proliferation and

Correspondence to: Professor Xu-Dong Zhao, Key Laboratory of Animal Models and Human Disease Mechanisms of Chinese Academy of Sciences and Yunnan Province, Kunming Institute of Zoology, Chinese Academy of Sciences, 21 Qingsong Road, Kunming, Yunnan 650223, P.R. China
E-mail: zhaoxudong@mail.kiz.ac.cn

Professor Rong-Tao Li, Faculty of Life Science and Technology, Kunming University of Science and Technology, 727 South Jingming Road, Kunming, Yunnan 650500, P.R. China
E-mail: rongtaolikm@163.com

*Contributed equally

Key words: rupesin E, glioma stem cells, proliferation, apoptosis, colony formation

multidirectional differentiation, with the basic characteristics of stem cells, known as tumor stem cells (11-13). They maintain the growth and proliferation of the tumor (14-16). In 2002, a type of cell with stem cell properties was identified in glioma, which was subsequently termed cancer stem cell (17). The discovery of the cancer stem cell provided a new idea for the treatment of tumors (18-20). Therefore, multiple studies have been performed using GSCs and demonstrated that they were closely associated with chemotherapy and radiotherapy resistance (6-9,15,21,22). In addition, GSCs were associated with promoting tumor angiogenesis (23,24), hypoxia response (25,26), tumor invasion and recurrence (27); thus, GSCs serve an important role in tumor growth and development. Therefore, GSCs may be a good target for the treatment of glioblastoma. Natural products have always been an important source of antitumor drugs (28,29), and isolated compounds have provided an important value for the development of antitumor drugs, such as, taxol and irinotecan. *Valeriana jatamansi* can relieve pain and diarrhea, reduce temperature and anxiety (30). It is mainly distributed in the southwest of China and used for the treatment of epigastric distension pain, dysuria, diarrhea, dysentery, rheumatalgia, lower back and knee tenderness and insomnia (31,32). Rupesin E is an iridoid isolated from the roots and rhizomes of *Valeriana jatamansi*. In a preliminary study, the screening results indicated that rupesin E may be selectively sensitive to GSCs. In order to confirm the activity and mechanism of rupesin E against GSCs, further experiments were performed to determine the proliferation, apoptotic, clone formation ability of GSCs after the treatment of rupesin E.

Materials and methods

Materials. Rupesin E was provided by Dr Rongtao Li from Kunming University of Science and Technology (Yunnan, China). Laminin (cat. no. 23017-015; Gibco; Thermo Fisher Scientific, Inc.), B27 supplement (cat. no. 12587-010; Gibco; Thermo Fisher Scientific, Inc.), Dulbecco's modified Eagle's Medium (DMEM; cat. no. 12800-017; Gibco, Thermo Fisher Scientific, Inc.), DMEM/F12 (cat. no. 11330-032; Gibco; Thermo Fisher Scientific, Inc.), PBS (cat. no. 18912-014; Gibco; Thermo Fisher Scientific, Inc.), fetal bovine serum (cat. no. 10099-141; Gibco; Thermo Fisher Scientific, Inc.), TryplE express (cat. no. 12604-021; Gibco) and 5-ethynyl-2'-deoxyuridine (EdU; Click-iT EdU Alexa Fluor 488 imaging kit; cat. no. C10337; Invitrogen) were purchased from Thermo Fisher Scientific, Inc. BSA (cat. no. FC0077) was purchased from MP Biomedicals, LLC. Goat serum (cat. no. C-0005) was purchased from Shanghai Haoran Biotechnology Co., Ltd. MTS[3-(4,5-dimethylthiazol-2-yl)-5-(3-carboxymethoxyphenyl)-2-(4-sulfophenyl)-2H-tetrazolium; cat. no. G3581] was purchased from Promega Corporation. Tween-20 (cat. no. SLBX6047) was purchased from Sigma-Aldrich; Merck KGaA. Low-gelling temperature agarose (cat. no. A9045) was purchased from was purchased from Sigma-Aldrich; Merck KGaA. The Annexin V-FITC Apoptosis Assays kit (cat. no. A005-4) was purchased from 7sea biotech. The basic fibroblast growth factor (bFGF; cat. no. AF-100-18B) and epidermal growth factor (EGF; cat. no. AF-100-15) were purchased from PeproTech, Inc. Primary anti-cleaved caspase-3 antibody (rabbit anti-cleaved caspase-3; cat. no. 9661) was obtained from Cell Signaling Technology, Inc. Anti-caspase-3 secondary antibody (Goat anti-rabbit IgG Fc Dylight-488; ab98462) was obtained from Abcam. Primary nestin antibody (cat. no. sc-23927) was purchased from Santa Cruz Biotechnology, Inc. Primary glial fibrillary acidic protein antibody (GFAP; cat. no. 20334) was purchased from Dako (Agilent Technologies, Inc). Primary GAPDH antibody (cat. no. ab9484) was obtained from Abcam. Goat anti-mouse IgG secondary antibody (cat. no. cw0102) was obtained from CWBio. Goat anti-rabbit IgG secondary antibody (cat. no. A6154) was obtained from Sigma-Aldrich (Merck KGaA). Flow cytometry (LSR Fortessa) was obtained from Becton, Dickinson and Company. The software used for the flow cytometry was the BD FACS Diva Software v8.0.1 (Becton, Dickinson and Company). Automatic chemiluminescence imaging analysis system (cat. no. Tanon-5200) was purchased from Shanghai Tianneng Technology Co. Ltd. The digital camera (Canon-1500D) was obtained from Canon, Inc.

Isolation and purification of Rupesin E. Rupesin E was isolated from the roots and rhizomes of *Valeriana jatamansi* by Dr Rongtao Li from Kunming University of Science and Technology (Yunnan, China). Firstly, the air-dried and powdered *Valeriana jatamansi* (25 kg) were extracted with 95% ethanol (3x37 l, 24 h each time) at room temperature and concentrated under vacuum to obtain a crude extract (2.7 kg), which was suspended in water and extracted successively with petroleum ether, ethyl acetate and n-butanol. The ethyl acetate extract (340 g) was subjected to silica gel column chromatography (CC; polyethylene/acetone; gradient, 1:0 to 0:1) to yield the eluted fractions E1 - E7. E4 (40.2 g) was isolated by CC over MCI gel (MCI gel is a highly porous styrene-divinylbenzene polymer resin used as column packing material; methanol/water; gradient, 30, 60, 70, 90 and 100%), silica gel (petroleum ether/acetone 30:1 to 5:1), Sephadex LH-20 (chloroform/methanol 1:1) and semi-preparative high performance liquid chromatography [HPLC; at 40˚C; sample quantity, 50 μl; using a Zorbax SB-C18 column (5 μm; 4.6x150 mm; Agilent Technologies, Inc.); 20% methanol/water; flow rate, 3 ml/min)] to yield rupesin E [181 mg, with a retention time (t_R; the time elapsed between sample introduction at the beginning of the chromatogram and the maximum signal of the given compound at the detector) of 14.3 min and purity of 98.1%]. A total of 10 mg rupesin E was dissolved in 1 ml DMSO to make a 10 mg/ml stock solution and stored at -20˚C, protected from light. The purity of the compound was analyzed using an Agilent 1260 HPLC system (at 40˚C; sample quantity, 50 μl) with a Zorbax SB-C18 (5 μm; 4.6 x 150 mm; Agilent Technologies, Inc.) column. The solvent system was methanol/water, gradient at the flow rate of 3 ml/min for 15 min. The structure of rupesin E was identified by comparison of the spectroscopic data with previously published values (33-36).

Cells and culture. The HAC (Human Astrocytes-cerebellar; cat. no. 1810) cell line was purchased from ScienCell Research Laboratories, Inc. and cultured in DMEM with 10% FBS. The three human GSC lines (GSC-3#, GSC-12# and GSC-18#) used were established from three different human glioblastoma samples by Kunming Institute of Zoology (Yunnan, China) that was obtained from Yunnan Cancer Hospital

(Kunming, China) (37,38). Tumor stem cells were cultured in GSC medium that consisted of DMEM/F12, 1 x B27, 50 ng/ml bFGF and 50 ng/ml EGF supplemented with 100 U/ml penicillin and 100 μg/ml streptomycin. In addition, the three human GSC lines were cultured in pre-coated culture dishes with laminin, and the cells could attach and grow normally without differentiation. Culture dishes were pre-coated with 10 μg/ml laminin for 6-9 h at 37˚C in a humidified incubator, dissociated with TryplE express for 5 min at 37˚C in a humidified incubator and centrifuged at 800 x g, at 25˚C for 5 min. The cells were suspended, and $1x10^6$ cells/ml were seeded into the pre-coated dishes and maintained at 37˚C in a humidified incubator with 5% CO_2. Human patient-derived GSCs, termed GSC-3#, GSC-12# and GSC-18#, were established as described before (39-42).

Morphological observation. The morphology of 10 μg/ml rupesin E-treated GSCs (GSC-3#, GSC-12# and GSC-18#) at 72 h after treatment was examined using an Olympus-IX71 light microscope (Olympus Corporation) and images were captured using an Olympus-DP72 (Olympus Corporation; magnification, x40).

MTS assay. A total of $2x10^4$ HAC and $2x10^4$ GSCs (GSC-3#, GSC-12# and GSC-18#) in 150 μl per well were seeded into 96-well plates and treated with 50 μl rupesin E at 80, 40, 20, 10, 5 and 2.5 μg/ml or 40, 20, 10, 5, 2.5 and 1.25 μg/ml, respectively. In a screening experiment, the effect of rupesin E on proliferation was stronger in glioma stem cells compared with that in HAC cells for 72 h. Therefore, the four cell lines were treated with different concentrations of rupesin E to obtain the IC_{50} values. HAC and GSCs that were treated with the same volume of DMSO (0.2%) were used as a normal control. All groups of cells were incubated for 72 h at 37˚C with 5% CO_2 after treatment with rupesin E. MTS reagent was diluted 1:10 with fresh complete medium and mixed thoroughly (43). The old medium was removed and 100 μl/well fresh medium was added. Compared with GSCs, HAC has higher metabolism and dehydrogenase activity, and can completely react with substrate in a shorter time and thus, GSCs were incubated for 1.5 h, whereas the HAC cells were incubated for 30 min, and the absorbance was measured using a BioTek synergy H1 microplate Hybrid Reader (BioTek Instruments, Inc.) at 490 nm. The viability of cells treated with rupesin E was compared with the control group treated with DMSO and expressed as a percentage. The half-maximal inhibitory concentration (IC_{50}) was calculated using Graph Pad Prism v5 software (GraphPad Software, Inc).

Cell proliferation assay. Cell proliferation assay was performed using 5-ethynyl-2'-deoxyuridine (EdU) immunofluorescence staining, as previously reported (44). The results were consistent in all three cell lines (GSC-3#, GSC-12# and GSC-18#) and the two of these cell lines were randomly selected. GSC-3# and GSC-18# were digested with TryplE express and seeded onto a 24-well plate with $1x10^5$ cells/per well. Rupesin E 10 μg/ml was added and the control wells were treated with the same volume of DMSO (0.2%). The GSC-3# cells were treated for 14 h and the GSC-18# cells were treated for 12 h at 37˚C in a humidified incubator. The GSCs were treated with EdU (10 μM) for 1 h at 37˚C in a humidified incubator with 5% CO_2. Following incubation, the media was removed and 500 μl 4% paraformaldehyde (PFA) was added to each well containing coverslips. The plate was incubated for 15 min at room temperature, following which the fixative was removed and the cells were washed twice with 1 ml 3% BSA in PBS. Once the wash solution was removed, 500 μl 0.5% Triton X-100 in PBS was added to each well, incubated at room temperature for 20 min and subsequently washed twice with 3% BSA. A total of 200 μl 1X Click-iT reaction mixture was added to each well, the plate was briefly agitated to ensure that the reaction mixture is distributed evenly over the coverslip and incubated for 30 min at room temperature protected from light. The reaction mixture was removed, and each well was washed twice with 1 ml 3% BSA in PBS and incubated with DAPI (10 mM; diluted 1:1,000 in PBS) for 10 min in the dark. The cells were washed twice with PBS and mounted onto a glass slide. Images were obtained using an Olympus IX71 (Olympus Corporation) fluorescent microscope at the magnifications x20 and x40.

Apoptosis assay. Apoptosis assay was performed using cleaved caspase-3 immunofluorescence staining. GSC-3# and GSC-18# cells ($1x10^5$ cells/well) were plated in 24-well culture dishes. The GSC-3# cells were treated with 10 μg/ml rupesin E for 39 h and the GSC-18# cells were treated with 10 μg/ml rupesin E for 14 h. A total of 500 μl 4% PFA was added to each well containing the coverslips and incubated for 20 min, followed by washing with 0.3% Triton X-100 three times. The cells were blocked with 10% goat serum (diluted in PBS) for 1 h at room temperature. Each well was incubated with primary anti-cleaved caspase-3 antibody (rabbit anti-cleaved caspase3; diluted 1:400 in PBS with 1% BSA and 0.25% Tween-20) for 1 h at room temperature and washed with 0.2% Tween-20 four times. The wells were incubated with anti-caspase3 secondary antibody (goat anti-rabbit IgG Fc Dylight-488; diluted 1:500 in PBS buffer with 1% BSA and 0.5% Tween-20) for 1 h away from light at room temperature. Each coverslip was washed with 0.2% Tween-20 4 times and incubated with DAPI (1:5,000 at 1 mg/ml) for 10 min in the dark, and the slides were washed with PBS three times and mounted onto glass slide. Images were obtained using an Olympus IX71 (Olympus Corporation) fluorescent microscope at the magnification of x20 and x40.

To further confirm these results, apoptosis assay was also performed using Annexin V/propidium iodide (PI) staining and analyzed using flow cytometry. GSC-3# cells ($8x10^5$) were plated in 6-well culture dishes. The cells were treated with either 10 μg/ml rupesin E or the same volume of DMSO (0.2%) as a control for 2, 4 and 8 h. Cells were digested using trypsin, collected and centrifugated at 500 x g for 5 min at 25˚C, following which the supernatant was discarded, and the pellet was gently resuspended with 1 ml PBS and centrifuged again at 500 x g for 5 min at 25˚C. A total of 400 μl 1X binding buffer was added to resuspend the cells, incubated with 5 μl Annexin V-FITC for 15 min in the dark at 4˚C, and 10 μl PI was added, placed on ice and protected from light. Flow cytometry analysis was performed within 30 min.

Western blot analysis. GSC-3# cells were treated with or without 10 μg/ml rupesin E (10 h), collected and lysed in

RIPA buffer (cat. no. R0010; Beijing Solarbio Science and Technology Co., Ltd.) with 0.1 mg/ml phenylmethylsulfonyl fluoride and phosphatase inhibitor. This was followed by centrifugation at 20,000 x g for 30 min at 4˚C. The protein precipitate was removed and the protein in the supernatant was quantified using the BCA assay kit (cat. no. P0010; Beyotime Institute of Biotechnology), denatured at 95˚C for 5 min and loaded onto 10% SDS-PAGE (50 μg per lane). Following electrophoresis, proteins were transferred to polyvinylidene fluoride membranes (EMD Millipore). The membranes were blocked for 1.5 h at room temperature in blocking buffer (5% skimmed milk in PBS with 0.2% Tween-20) and incubated with the primary antibodies [Nestin and glial fibrillary acidic protein (GFAP) were diluted to 1:500, GAPDH to 1:1,000] overnight at 4˚C. Following washing with 0.1% Tween-20 in PBS three times, the membranes were incubated with either goat anti-rabbit IgG secondary antibody (1:10,000 dilution), or goat anti-mouse IgG secondary antibodies (1:10,000 dilutions) for 2 h at room temperature. Finally, the membranes were treated with Automatic chemiluminescence imaging analysis system (Tanon-5200) and exposed to ECL. Results were analyzed using Image J Software (National Institutes of Health). GAPDH was used as a reference gene.

Soft agar colony formation assay. The soft agar colony formation assay was performed as previously described (45,46). The low gelling agar (0.4 g) was mixed with 13 ml double distilled water and sterilized by high-pressure steam sterilization (121˚C, 15 min) to make 3.2% soft agar. To prepare the 0.8% bottom layer of agar, 3.2% soft agar was diluted 1:4 in GSC medium and plated in a 6-well-plate at 1 ml/well. The plates were left at room temperature to cool. To prepare the 0.4% upper layer of agar, GSC-3# and GSC-18# were digested with TryplE express and $2x10^4$ cells/well were mixed with 0.8% agar to 0.4% concentration and plated in a 6-well-plate at 1 ml/well, cooled and supplemented with 1 ml GSC medium. The plates were cultured in a cell incubator (at 37˚C in a humidified incubator with 5% CO_2) and fresh medium was added every 3-4 days. After two weeks, once the clonal spheres had reached a certain size (20 μm), they were treated with 20 μg/ml rupesin E every 3 days. The control groups were treated with the same volume of 0.2% DMSO and fresh medium was added every 3 days. After two weeks, the GSC medium was removed and washed once with PBS. The clonal spheres were fixed with 1 ml 4% PFA at room temperature containing 0.005% crystal violet for 2 h. Images were obtained using a digital camera and the clonal spheres were counted.

Statistical analysis. All data were expressed as the means ± standard error of the mean of three separate experiments. GraphPad Prism v5.0 software (GraphPad Software, Inc.) was used for statistical analysis. One-way analysis of variance followed by the least significant difference post hoc test was used to determine statistical significance. $P<0.05$ was considered to indicate a statistically significant difference.

Results

Structure identification of rupesin E. ^{1}H-NMR spectrum (deuterated acetone; 600 MHz) of rupesin E is presented in Fig. S1 and ^{13}C-NMR spectrum (deuterated acetone; 150 MHz) of compound rupesin E is presented in Fig. S2. The ^{1}H-NMR and ^{13}C-NMR data of Rupesin E are as follows and consistent to those of the references (33-36).

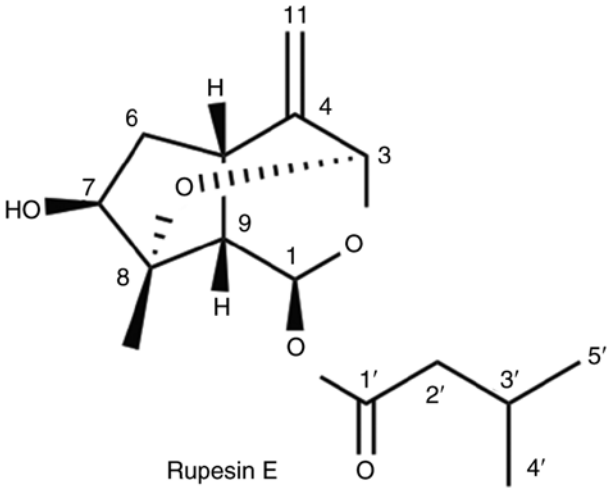

Figure 1. Structural formula of rupesin E.

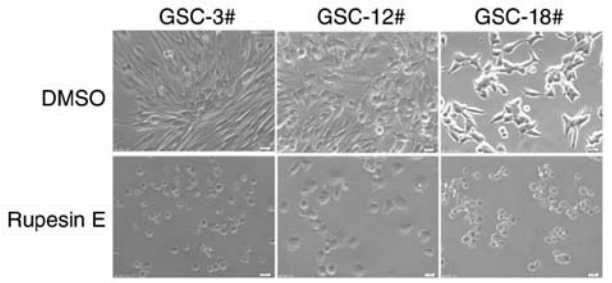

Figure 2. Morphology of rupesin E treatment on GSC-3#; GSC-12# and GSC-18# viability at 10 μg/ml (magnification, x40), the cell plasma membrane was blebbing and cells were detached. GSC, glioma stem cell.

Rupesin E, colorless oil, $C_{15}H_{22}O_5$, ^{1}H-NMR (CD_3COCD_3; 600 MHz): δH 6.28 (1H, d, J=3.2 Hz, H_a-1), 5.03 (1H, s, H-3), 3.12-3.10 (1H, m, H-5), 2.08-2.00 (1H, overlap, H_a-6), 1.90-1.86 (1H, m, H_b-6), 3.85-3.80 (1H, m, H-7), 4.20 (1H, br s, OH-C-7), 2.41-2.39 (1H, m, H-9), 1.36 (3H, s, H-10), 4.87 (1H, s, H_a-11), 4.80 (1H, s, H_b-11), 2.19-2.11 (2H, m, H-2'), 2.08-2.00 (1H, overlap, H-3'), 0.92 (3H, d, J=4.5 Hz, H-4'), 0.91 (3H, d, J=4.5 Hz, H-5'). ^{13}C-NMR (CD_3COCD_3; 150 MHz): δC 90.7 (CH, C-1), 94.3 (CH, C-3), 150.4 (C, C-4), 37.5 (CH, C-5), 43.8 (CH_2, C-6), 79.0 (CH, C-7), 83.0 (C, C-8), 42.5 (CH, C-9), 19.2 (CH_3, C-10), 107.2 (CH_2, C-11), 171.9 (C, C-1'), 43.5 (CH_2, C-2'), 26.1 (CH, C-3'), 22.5 (C, C-4'), 22.4 (CH, C-5').

Rupesin E selectively inhibits the viability of GSCs. In a screening experiment, the proliferation-inhibiting efficacy of rupesin E (Fig. 1) against three human GSC lines (GSC-3#, GSC-12# and GSC-18#) was evaluated. At 10 μg/ml, rupesin E inhibited the proliferation of all GSCs effectively, based on morphological observation (Fig. 2). In addition, the inhibitory effect of rupesin E on the viability of GSCs and normal human HAC cells was investigated using an MTS assay at varying concentrations of rupesin E (40, 20, 10, 5,

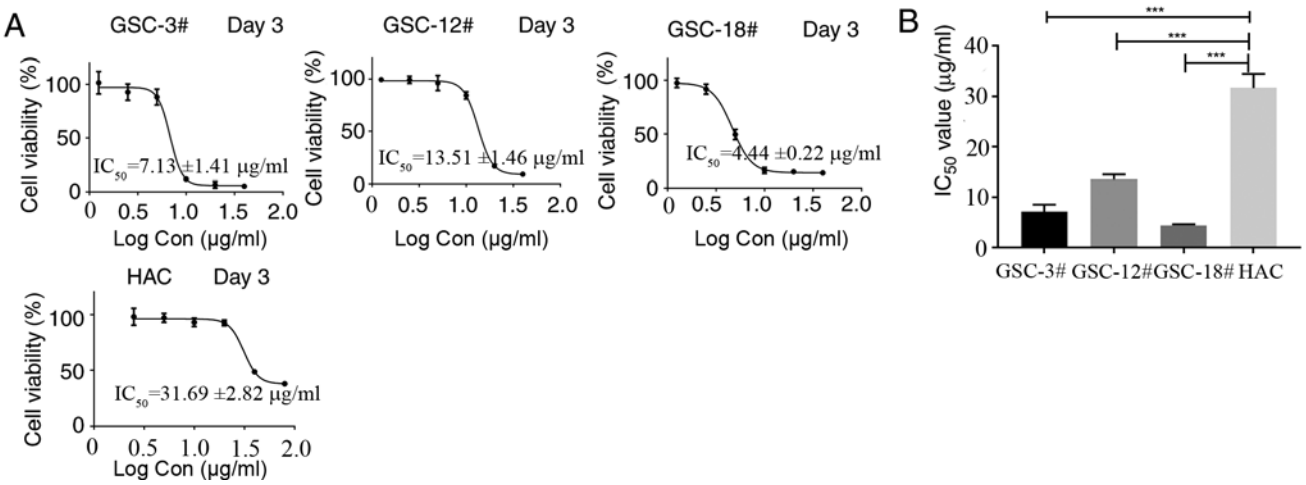

Figure 3. Cell viability and IC_{50} value for GSCs and HAC cell line. (A) The cell viability and IC_{50} value was measured using the MTS assay. (B) The quantitative data of IC_{50}. ***P<0.001. GSCs, glioma stem cells; HAC, human astrocytes-cerebellar.

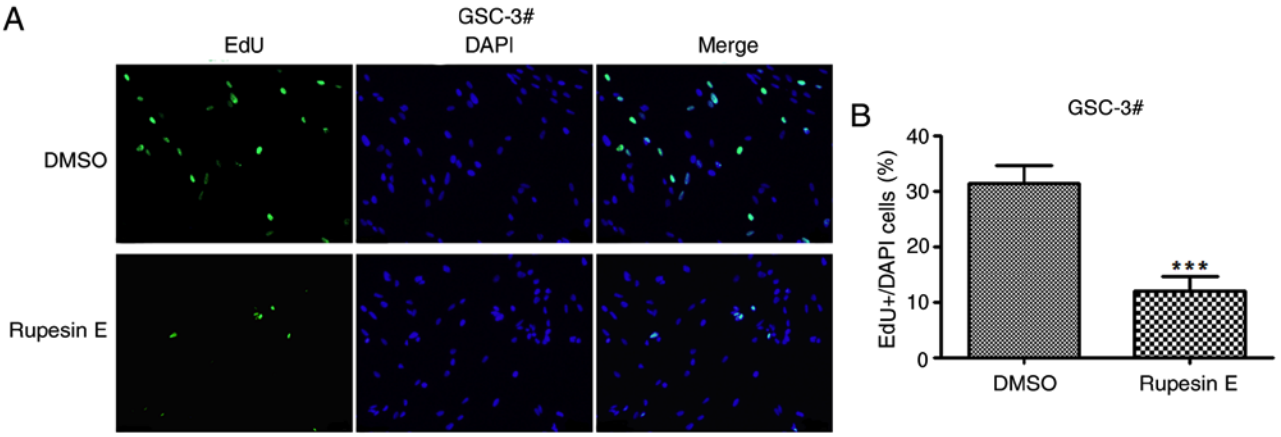

Figure 4. Rupesin E suppresses GSC-3# proliferation. (A) Cell proliferation was measured using the EdU assay (magnification, x40). (B) The quantitative data of panel A. ***P<0.001. EdU, 5-ethynyl-2'-deoxyuridine. GSC, glioma stem cells.

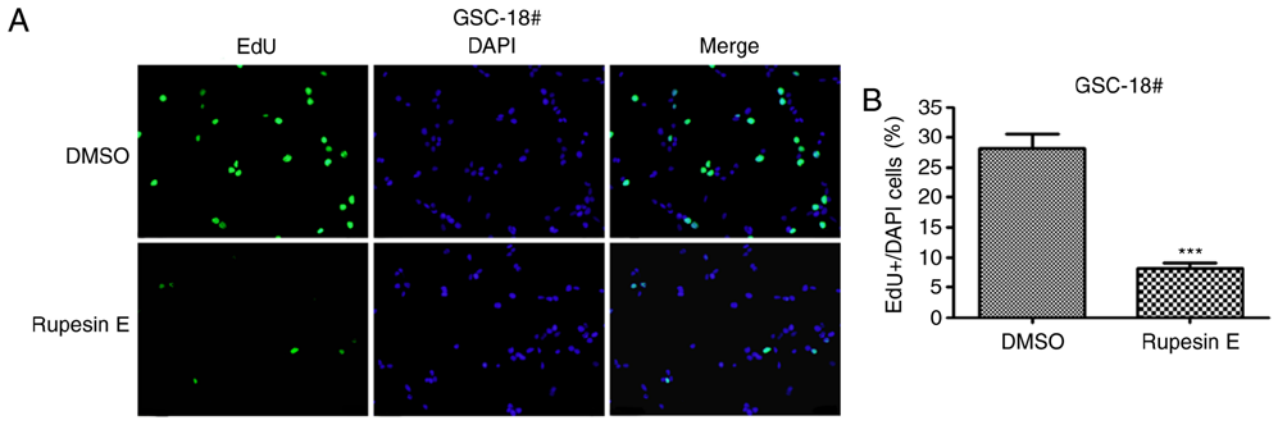

Figure 5. Rupesin E suppresses GSC-18# proliferation. (A) Cell proliferation was measured using the EdU assay (magnification, x40). (B) The quantitative data of panel A. ***P<0.001. GSC, glioma stem cells.

2.5 and 1.25 μg/ml in GSCs; 80, 40, 20, 10, 5 and 2.5 μg/ml in HAC cells) after treatment for 72 h. As shown in Fig. 3, rupesin E inhibited the viability of human GSCs and HAC cells in a concentration-dependent manner. The half maximal inhibitory concentration (IC_{50}) values of rupesin E in human GSCs (GSC-3#, GSC-12# and GSC-18#) were 7.13±1.41, 13.51±1.46 and 4.44±0.22 μg/ml at 72 h, respectively. For the HAC cells, the IC_{50} value was 31.69±2.82 μg/ml for 72 h. These

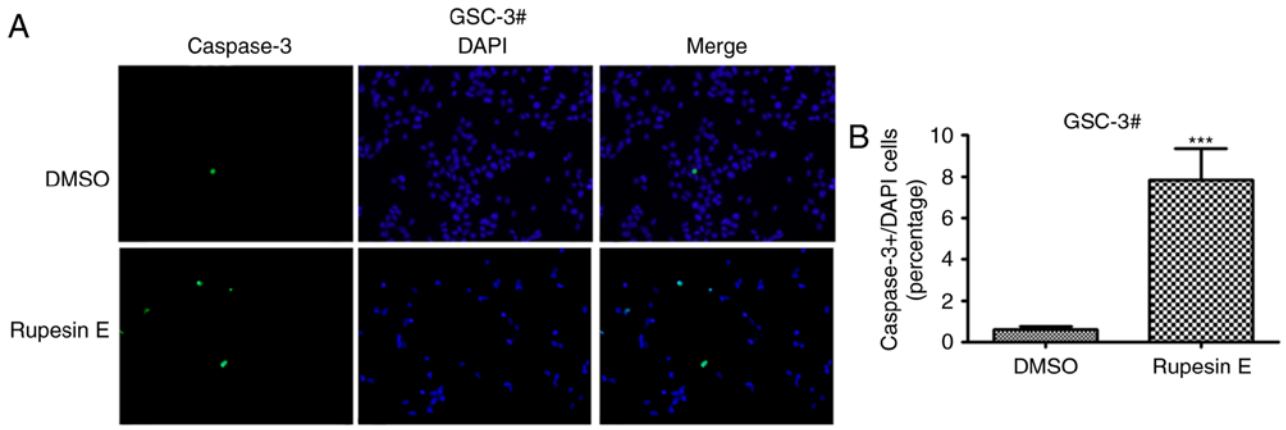

Figure 6. Rupesin E induces GSC-3# apoptosis via cleaved caspase-3. (A) Cell apoptosis was measured using cleaved-caspase-3 immunofluorescence staining (magnification, x40). (B) The quantitative data of panel A. ***P<0.001. GSC, glioma stem cells.

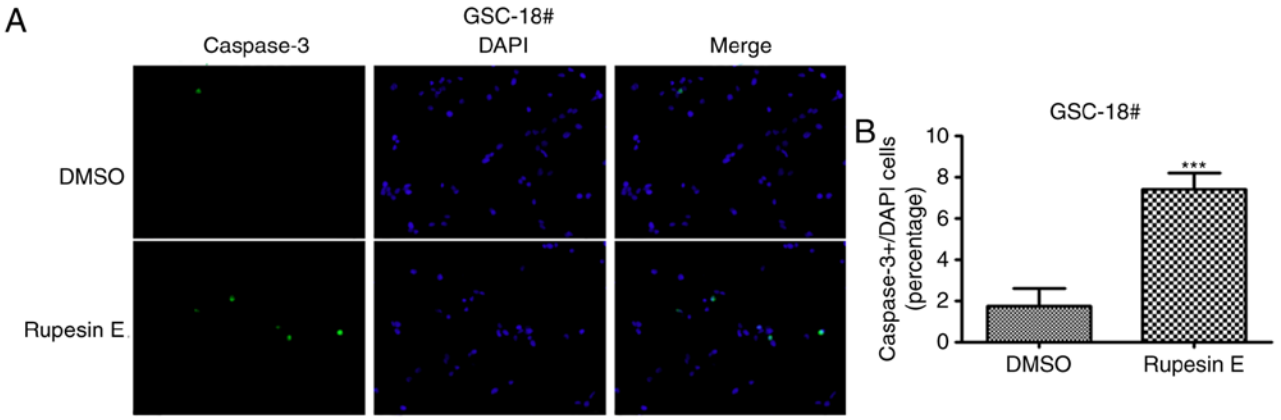

Figure 7. Rupesin E induces GSC-18# apoptosis via cleaved caspase-3. (A) Cell apoptosis was measured using cleaved-caspase-3 immunofluorescence staining (magnification, x40). (B) The quantitative data of panel A. ***P<0.001. GSC, glioma stem cells.

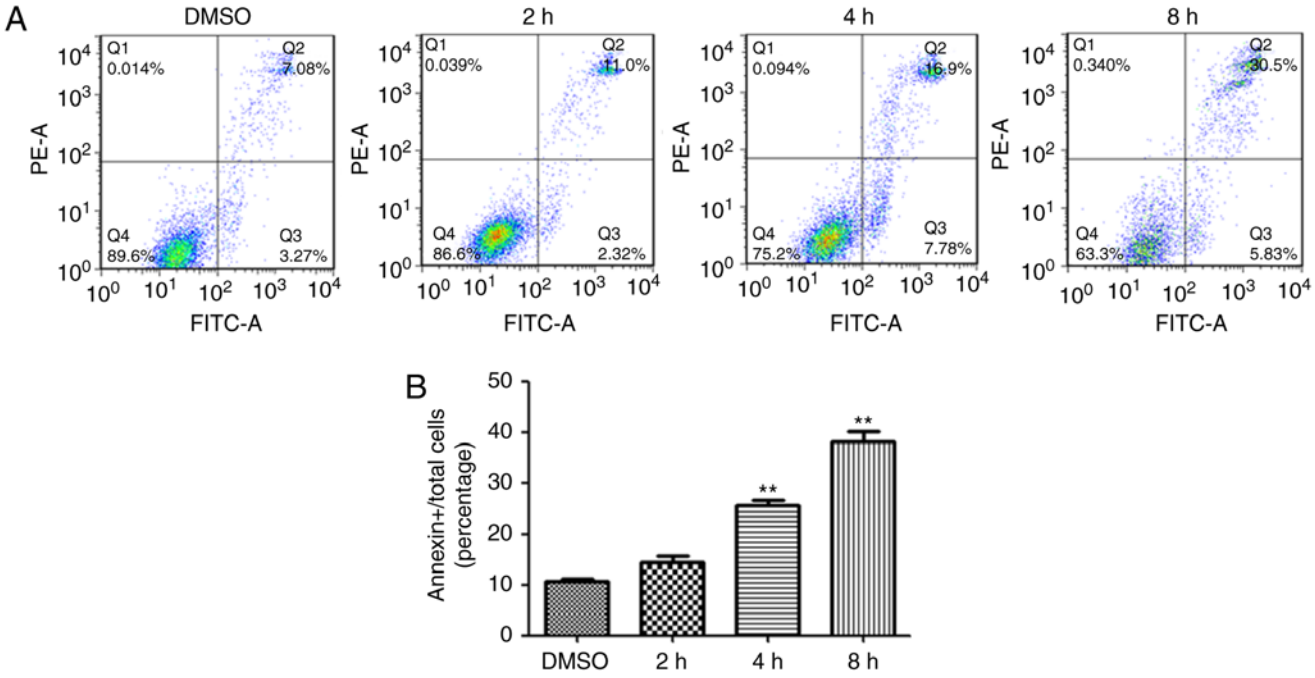

Figure 8. Rupesin E induces GSC-3# apoptosis. (A) GSC-3# were treated with rupesin E (2, 4 or 8 h), stained with Annexin V-FITC/PI and analyzed using flow cytometry. (B) The quantitative data of panel A. Percentages of Annexin-V positive apoptotic cells vs. total cells are shown. **P<0.01. PI, propidium iodide; GSC, glioma stem cells.

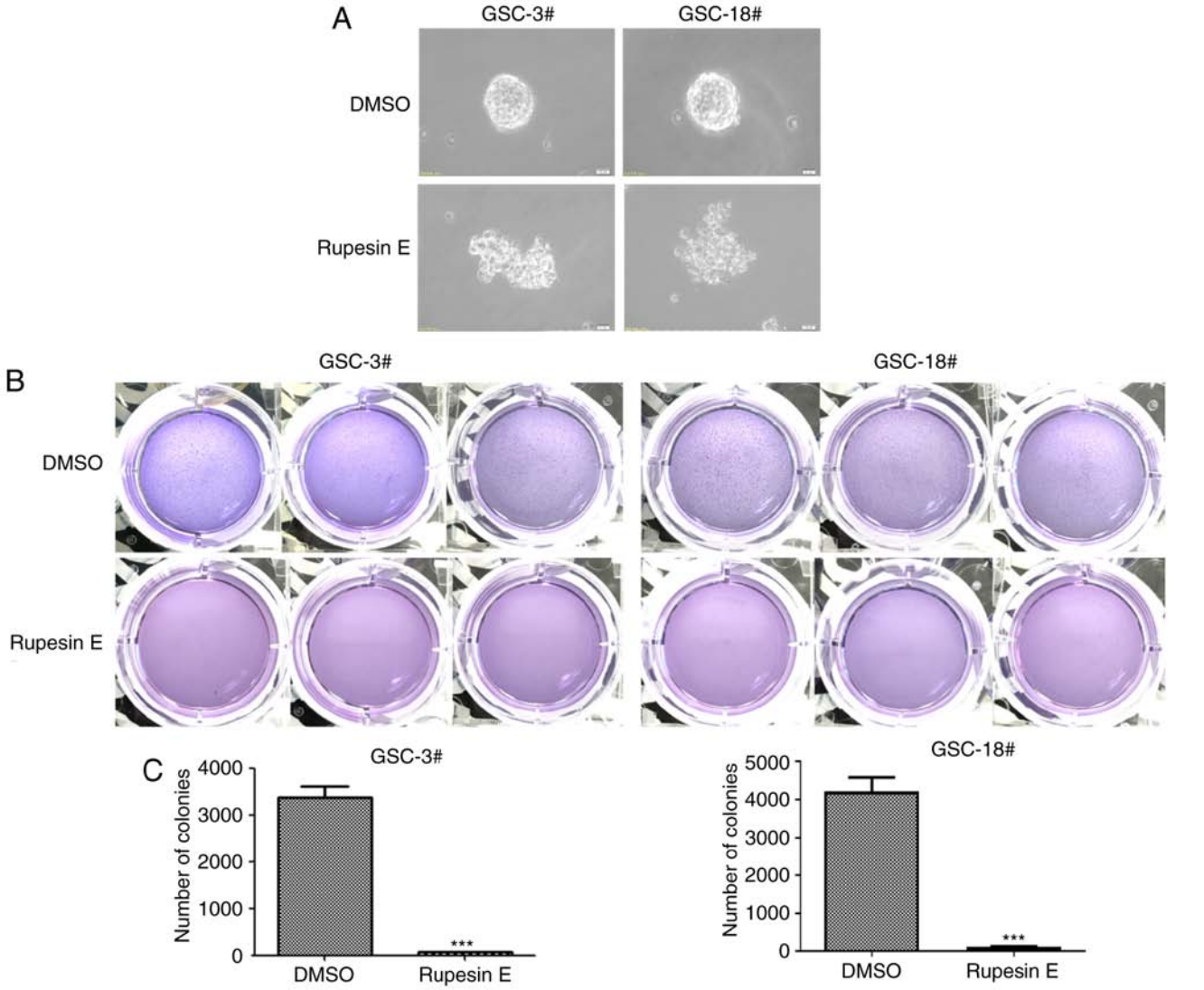

Figure 9. Rupesin E damages GSC colony formation. (A) GSC-3# and GSC-18# clonal sphere morphology was damaged following treatment with rupesin E (magnification, x40). (B) GSC-3# and GSC-18# clonal spheres were stained with 4% paraformaldehyde and 0.005% crystal violet for 2 h. (C) The quantitative data of GSC-3# and GSC-18# in panel B. The numbers of clonal spheres are shown. ***P<0.001. GSC, glioma stem cell.

results indicated that GSCs were more sensitive to rupesin E compared with HAC cells.

Rupesin E suppresses the proliferation of GSCs. In the preliminary experiment, rupesin E was identified to inhibit the proliferation of GSCs; however, its mechanism of action is unknown. To determine whether rupesin E suppressed cell proliferation by suppressing DNA synthesis, GSC-3# and GSC-18# were subjected to EdU incorporation assay and treated with rupesin E (10 μg/ml) for 14 and 12 h, respectively (Figs. 4 and 5). The results demonstrated that the percentage of Edu-positive proliferative cells significantly decreased in cells treated with rupesin E compared with that in the control group. This indicated that rupesin E notably inhibited cell proliferation through the suppression of DNA synthesis in the two GSC lines.

Rupesin E induces apoptosis of GSCs. The treatment of rupesin E resulted in the decline of cell viability in both GSC-3# and GSC-18#, and the cells became spherical and detached, which

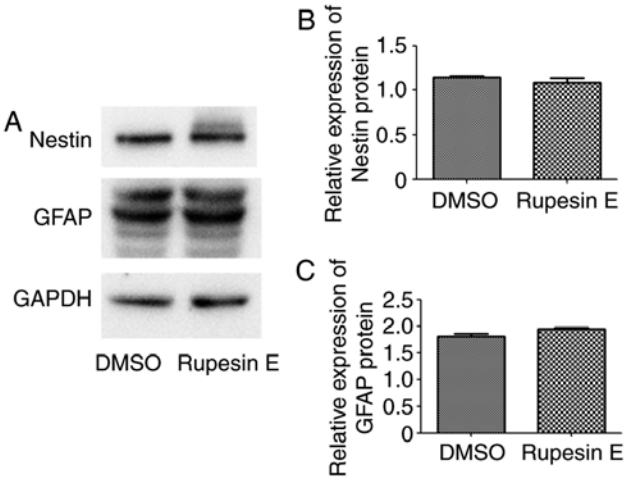

Figure 10. Differentiation-related protein expression following treatment with Rupesin E. (A) The protein expression level of nestin and GFAP in GSC-3# treated with DMSO was similar to that in GSC-3# treated with 10 μg/ml rupesin E (10 h). Quantitative analysis of (B) nestin and (C) GFAP protein expression levels in GSC-3#. GSC, glioma stem cells.

suggested that rupesin E may induce apoptosis in GSCs. To determine whether GSCs underwent apoptosis after the treatment of rupesin E, the level of apoptosis in GSC-3# and GSC-18# was measured using immunofluorescent staining. The activation of caspase-3 occurs in the early stage of apoptosis, which was significantly increased in both GSC-3# (Fig. 6) and GSC-18# (Fig. 7) treated with rupesin E (10 μg/ml) for 39 and 14 h, respectively. In addition, the level of apoptosis was further measured using Annexin V/PI assay and flow cytometry in GSC-3#. The result demonstrated that the proportions of Annexin V-positive apoptotic cells were increased significantly in GSC-3# compared with the control after 4 and 8 h treatment with rupesin E (Fig. 8). These results revealed that rupesin E induced apoptosis of GSC-3# and GSC-18#.

Rupesin E inhibits the colony formation ability of GSCs. To examine whether rupesin E inhibited the proliferative ability of GSCs, the colony formation assay was performed to determine the ability of the single cell to divide unlimitedly following the treatment of a cytotoxic agent *in vitro*. GSC-3# and GSC-18# were seeded in the soft agar and once the clonal spheres achieved a certain size (20 μm), rupesin E (20 μg/ml) was used to treat GSCs. The results demonstrated that rupesin E significantly reduced the number of clonal spheres (Fig. 9), thus reducing the ability of GSCs to divide unlimitedly.

Rupesin E does not induce the differentiation of GSCs. Nestin is a well-established marker of GSC stemness, and GFAP is widely used as the differentiation marker of GSCs (47). GSC-3# cells were treated with 10 μg/ml rupesin E for 10 h, following which the protein expression of nestin and GFAP were detected using western blot analysis. The results demonstrated that after rupesin E treatment, the expression of nestin did not significantly decline and the expression of GFAP did not significantly increase (Fig. 10); these results indicated that rupesin E could not induce GSC differentiation.

Discussion

The limitations of surgical treatment make it impossible to completely remove tumors (5), and chemotherapy and radiotherapy are only effective on rapidly dividing tumor cells. As the cancer stem cells are tolerant to chemotherapy and radiotherapy, chemotherapy and radiotherapy are ineffective against it (39). GSCs and normal stem cells exhibit the same features, such as infinite proliferation, self-renewal and the cloning expansion ability to form tumors, which may be important reasons for tumor recurrence (17), which was also demonstrated in the current study. This also provides the theoretical basis for this study. Therefore, a large number of studies aim to identify compounds that specifically target glioma stem cells from small molecular compounds (48-50). However, no drugs specifically targeting cancer stem cells have been marketed to date. In the present study, a high-throughput screening of 3,000 small-molecule compounds was conducted, and it was found that rupesin E could selectively inhibit glioma stem cells. Using the same concentration, rupesin E reduced proliferation and induced apotosis of GSCs and had no effect on the proliferation of HAC cells. In addition, rupesin E not only induced GSC apoptosis, but also inhibited GSC ability of infinite proliferation. Thus, rupesin E has the potential to be developed as an antitumor agent, and combined with radiotherapy, chemotherapy and surgical treatment, to completely remove the tumor.

Acknowledgements

Not applicable.

Funding

The present study was partly supported by the National Natural Science Foundation of China (grant nos. 81472862, 31560103 and U1602222).

Availability of data and materials

All data generated or analyzed during the present study are included in this published article.

Authors' contributions

SQ and LQ performed the experiments and wrote the manuscript. RL and XZ designed the study and edited the manuscript. HL and XC collected and analyzed the data.

Ethics approval and consent for publication

Not applicable

Patient consent for publication

Not applicable.

Competing interests

The authors declare that they have no competing interests.

References

1. Louis DN, Ohgaki H, Wiestler OD, Cavenee WK, Burger PC, Jouvet A, Scheithauer BW and Kleihues P: The 2007 WHO classification of tumours of the central nervous system. Acta Neuropathol 114: 97-109, 2007.
2. Furnari FB, Fenton T, Bachoo RM, Mukasa A, Stommel JM, Stegh A, Hahn WC, Ligon KL, Louis DN, Brennan C, *et al*: Malignant astrocytic glioma: Genetics, biology, and paths to treatment. Genes Dev 21: 2683-2710, 2007.
3. Scott CB, Scarantino C, Urtasun R, Movsas B, Jones CU, Simpson JR, Fischbach AJ and Curran WJ Jr: Validation and predictive power of radiation therapy oncology group (RTOG) recursive partitioning analysis classes for malignant glioma patients: A report using RTOG 90-06. Int J Radiat Oncol Biol Phys 40: 51-55, 1998.
4. Visser O, Ardanaz E, Botta L, Sant M, Tavilla A and Minicozzi P; EUROCARE-5 Working Group: Survival of adults with primary malignant brain tumours in Europe; results of the EUROCARE-5 study. Eur J Cancer 51: 2231-2241, 2015.
5. Alifieris C and Trafalis DT: Glioblastoma multiforme: Pathogenesis and treatment. Pharmacol Ther 152: 63-82, 2015.
6. Bao S, Wu Q, McLendon RE, Hao Y, Shi Q, Hjelmeland AB, Dewhirst MW, Bigner DD and Rich JN: Glioma stem cells promote radioresistance by preferential activation of the DNA damage response. Nature 444: 756-760, 2006.
7. Dean M, Fojo T and Bates S: Tumour stem cells and drug resistance. Nat Rev Cancer 5: 275-284, 2005.
8. Alisi A, Cho WC, Locatelli F and Fruci D: Multidrug resistance and cancer stem cells in neuroblastoma and hepatoblastoma. Int J Mol Sci 14: 24706-24725, 2013.

9. Chen J, Li Y, Yu TS, McKay RM, Burns DK, Kernie SG and Parada LF: A restricted cell population propagates glioblastoma growth after chemotherapy. Nature 488: 522-526, 2012.
10. Genadry KC, Pietrobono S, Rota R and Linardic CM: Soft tissue sarcoma cancer stem cells: An overview. Front Oncol 8: 475, 2018.
11. Codony-Servat J, Verlicchi A and Rosell R: Cancer stem cells in small cell lung cancer. Transl Lung Cancer Res 5: 16-25, 2016.
12. Johnsen HE, Bøgsted M, Schmitz A, Bødker JS, El-Galaly TC, Johansen P, Valent P, Zojer N, Van Valckenborgh E, Vanderkerken K, *et al*: The myeloma stem cell concept, revisited: From phenomenology to operational terms. Haematologica 101: 1451-1459, 2016.
13. Parte SC, Batra SK and Kakar SS: Characterization of stem cell and cancer stem cell populations in ovary and ovarian tumors. J Ovarian Res 11: 69, 2018.
14. Calabrese C, Poppleton H, Kocak M, Hogg TL, Fuller C, Hamner B, Oh EY, Gaber MW, Finklestein D, Allen M, *et al*: A perivascular niche for brain tumor stem cells. Cancer Cell 11: 69-82, 2007.
15. Koren E and Fuchs Y: The bad seed: Cancer stem cells in tumor development and resistance. Drug Resist Updat 28: 1-12, 2016.
16. Lathia JD, Mack SC, Mulkearns-Hubert EE, Valentim CL and Rich JN: Cancer stem cells in glioblastoma. Genes Dev 29: 1203-1217, 2015.
17. Ignatova TN, Kukekov VG, Laywell ED, Suslov ON, Vrionis FD and Steindler DA: Human cortical glial tumors contain neural stem-like cells expressing astroglial and neuronal markers in vitro. Glia 39: 193-206, 2002.
18. Bexell D, Svensson A and Bengzon J: Stem cell-based therapy for malignant glioma. Cancer Treat Rev 39: 358-365, 2013.
19. Bovenberg MS, Degeling MH and Tannous BA: Advances in stem cell therapy against gliomas. Trends Mol Med 19: 281-291, 2013.
20. Wang T, Shigdar S, Gantier MP, Hou Y, Wang L, Li Y, Shamaileh HA, Yin W, Zhou SF, Zhao X and Duan W: Cancer stem cell targeted therapy: Progress amid controversies. Oncotarget 6: 44191-44206, 2015.
21. Colak S and Medema JP: Cancer stem cells-important players in tumor therapy resistance. FEBS J 281: 4779-4791, 2014.
22. Lage H: An overview of cancer multidrug resistance: A still unsolved problem. Cell Mol Life Sci 65: 3145-3167, 2008.
23. Folkins C, Shaked Y, Man S, Tang T, Lee CR, Zhu Z, Hoffman RM and Kerbel RS: Glioma tumor stem-like cells promote tumor angiogenesis and vasculogenesis via vascular endothelial growth factor and stromal-derived factor 1. Cancer Res 69: 7243-7251, 2009.
24. Bao S, Wu Q, Sathornsumetee S, Hao Y, Li Z, Hjelmeland AB, Shi Q, McLendon RE, Bigner DD and Rich JN: Stem cell-like glioma cells promote tumor angiogenesis through vascular endothelial growth factor. Cancer Res 66: 7843-7848, 2006.
25. Pietras A, Gisselsson D, Ora I, Noguera R, Beckman S, Navarro S and Påhlman S: High levels of HIF-2alpha highlight an immature neural crest-like neuroblastoma cell cohort located in a perivascular niche. J Pathol 214: 482-488, 2008.
26. Li Z, Bao S, Wu Q, Wang H, Eyler C, Sathornsumetee S, Shi Q, Cao Y, Lathia J, McLendon RE, *et al*: Hypoxia-inducible factors regulate tumorigenic capacity of glioma stem cells. Cancer Cell 15: 501-513, 2009.
27. Plate KH and Risau W: Angiogenesis in malignant gliomas. Glia 15: 339-347, 1995.
28. Mondal S, Bandyopadhyay S, Ghosh MK, Mukhopadhyay S, Roy S and Mandal C: Natural products: Promising resources for cancer drug discovery. Anticancer Agents Med Chem 12: 49-75, 2012.
29. Moselhy J, Srinivasan S, Ankem MK and Damodaran C: Natural products that target cancer stem cells. Anticancer Res 35: 5773-5788, 2015.
30. Thies PW and Funke S: On the active ingredients in baldrian. 1. Detection and isolation of isovalerian acid esters with sedative effect from roots and rhizomes of various valerian and kentranthus species. Tetrahedron Lett 11: 1155-1162, 1966 (In German).
31. Thies PW: Linarin-isovalerianate, a currently unknown flavonoid from Valeriana wallichii D.C. 6. Report on the active substances of Valeriana. Planta Med 16: 363-371, 1968 (In German).
32. Thies PW: Valerosidatum, ein iridoidesterglycosid aus valeriana-arten 7. mitteilung über die wirkstoffe des baldrians. Tetrahedron Lett 11: 2471-2474, 1970.
33. Yang XP, Li EW, Zhang Q, Yuan CS and Jia ZJ: Five new iridoids from Patrinia rupestris. Chem Biodivers 3: 762-770, 2006.
34. Dong FW, Jiang HH, Yang L, Gong Y, Zi CT, Yang D, Ye CJ, Li H, Yang J, Nian Y, *et al*: Valepotriates from the roots and rhizomes of *Valeriana jatamansi* jones as Novel N-type calcium channel antagonists. Front Pharmacol 9: 885, 2018.
35. Dong FW, Liu Yang, Wu ZK, Wei-Gao, Zi CT, Dan Yang, Luo HR, Jun Zhou and Hu JM: Iridoids and sesquiterpenoids from the roots of *Valeriana jatamansi* jones. Fitoterapia 102: 27-34, 2015.
36. Lin S, Chen T, Liu XH, Shen YH, Li HL, Shan L, Liu RH, Xu XK, Zhang WD and Wang H: Iridoids and lignans from *Valeriana jatamansi*. J Nat Prod 73: 632-638, 2010.
37. Lee J, Kotliarova S, Kotliarov Y, Li A, Su Q, Donin NM, Pastorino S, Purow BW, Christopher N, Zhang W, *et al*: Tumor stem cells derived from glioblastomas cultured in bFGF and EGF more closely mirror the phenotype and genotype of primary tumors than do serum-cultured cell lines. Cancer cell 9: 391-403, 2006.
38. Wilson RJ, Thomas CD, Fox R, Roy DB and Kunin WE: Spatial patterns in species distributions reveal biodiversity change. Nature 432: 393-396, 2004.
39. Dai Z, Li SR, Zhu PF, Liu L, Wang B, Liu YP, Luo XD and Zhao XD: Isocostunolide inhibited glioma stem cell by suppression proliferation and inducing caspase dependent apoptosis. Bioorg Med Chem Lett 27: 2863-2867, 2017.
40. Wang B, Dai Z, Yang XW, Liu YP, Khan A, Yang ZF, Huang WY, Wang XH, Zhao XD and Luo XD: Novel nor-monoterpenoid indole alkaloids inhibiting glioma stem cells from fruits of Alstonia scholaris. Phytomedicine 48: 170-178, 2018.
41. Wei X, Dai Z, Yang J, Khan A, Yu HF, Zhao YL, Wang YF, Liu YP, Yang ZF, Huang WY, *et al*: Unprecedented sugar bridged bisindoles selective inhibiting glioma stem cells. Bioorg Med Chem 26: 1776-1783, 2018.
42. Yang XW, Dai Z, Wang B, Liu YP, Zhao XD and Luo XD: Antitumor triterpenoid saponin from the fruits of avicennia marina. Nat Prod Bioprospect 8: 347-353, 2018.
43. Chen J, Creed A, Chen AY, Huang H, Li Z, Rankin GO, Ye X, Xu G and Chen YC: Nobiletin suppresses cell viability through AKT pathways in PC-3 and DU-145 prostate cancer cells. BMC Pharmacol Toxicol 15: 59, 2014.
44. Ning H, Albersen M, Lin G, Lue TF and Lin CS: Effects of EdU labeling on mesenchymal stem cells. Cytotherapy 15: 57-63, 2013.
45. Borowicz S, Van Scoyk M, Avasarala S, Karuppusamy Rathinam MK, Tauler J, Bikkavilli RK and Winn RA: The soft agar colony formation assay. J Vis Exp: e51998, 2014.
46. Franken NA, Rodermond HM, Stap J, Haveman J and van Bree C: Clonogenic assay of cells in vitro. Nat Protoc 1: 2315-2319, 2006.
47. Bien-Möller S, Balz E, Herzog S, Plantera L, Vogelgesang S, Weitmann K, Seifert C, Fink MA, Marx S, Bialke A, *et al*: Association of glioblastoma multiforme stem cell characteristics, differentiation, and microglia marker genes with patient survival. Stem Cells Int 2018: 9628289, 2018.
48. Danovi D, Folarin A, Gogolok S, Ender C, Elbatsh AM, Engström PG, Stricker SH, Gagrica S, Georgian A, Yu D, *et al*: A high-content small molecule screen identifies sensitivity of glioblastoma stem cells to inhibition of polo-like kinase 1. PLoS One 8: e77053, 2013.
49. Hothi P, Martins TJ, Chen L, Deleyrolle L, Yoon JG, Reynolds B and Foltz G: High-throughput chemical screens identify disulfiram as an inhibitor of human glioblastoma stem cells. Oncotarget 3: 1124-1136, 2012.
50. Junca A, Villalva C, Tachon G, Rivet P, Cortes U, Guilloteau K, Balbous A, Godet J, Wager M and Karayan-Tapon L: Crizotinib targets in glioblastoma stem cells. Cancer Med 6: 2625-2634, 2017.

This work is licensed under a Creative Commons Attribution-NonCommercial-NoDerivatives 4.0 International (CC BY-NC-ND 4.0) License.